

Feasibility of simultaneous high-resolution anatomical and quantitative magnetic resonance imaging of sciatic nerves in patients with Charcot–Marie–Tooth type 1A (CMT1A) at 7T

Bragi Sveinsson PhD^{1,2} | Olivia E. Rowe BS^{1,2} | Jason P. Stockmann PhD^{1,2} |
 Daniel J. Park PhD¹  | Peter J. Lally PhD³ | Matthew S. Rosen PhD^{1,2,4} |
 Robert L. Barry PhD^{1,2,5} | Florian Eichler MD⁶ | Bruce R. Rosen MD, PhD^{1,2} |
 Reza Sadjadi MD⁶ 

¹Athinoula A. Martinos Center for Biomedical Imaging, Department of Radiology, Massachusetts General Hospital, Boston, Massachusetts, USA

²Department of Radiology, Harvard Medical School, Boston, Massachusetts, USA

³Department of Brain Sciences, Imperial College London, London, UK

⁴Department of Physics, Harvard University, Cambridge, Massachusetts, USA

⁵Harvard-Massachusetts Institute of Technology Health Sciences and Technology, Cambridge, Massachusetts, USA

⁶Department of Neurology, Massachusetts General Hospital, Harvard Medical School, Boston, Massachusetts, USA

Correspondence

Reza Sadjadi, Department of Neurology, Massachusetts General Hospital, Harvard Medical School, Boston, Massachusetts, USA.
 Email: rseyedsadjadi@mgh.harvard.edu

Funding information

Center for Functional Neuroimaging Technologies, Grant/Award Number: P41EB015896; Center for Mesoscale Mapping, Grant/Award Number: P41EB030006; National Institute of Health, Grant/Award Numbers: K99AG066815, R01EB027779, R01EB028797, S10OD023637; National Institutes of Health; National Institute of Biomedical Imaging and Bioengineering; Massachusetts General Hospital; Center for Biomedical Imaging; American Brain Foundation; American Academy of Neurology, Grant/Award Number: Clinical research scholarship (American Brain Foun

Abstract

Introduction/Aims: Magnetic resonance imaging (MRI) of peripheral nerves can provide image-based anatomical information and quantitative measurement. The aim of this pilot study was to investigate the feasibility of high-resolution anatomical and quantitative MRI assessment of sciatic nerve fascicles in patients with Charcot–Marie–Tooth (CMT) 1A using 7T field strength.

Methods: Six patients with CMT1A underwent imaging on a high-gradient 7T MRI scanner using a 28-channel knee coil. Two high-resolution axial images were simultaneously acquired using a quantitative double-echo in steady-state (DESS) sequence. By comparing the two DESS echoes, T2 and apparent diffusion coefficient (ADC) maps were calculated. The cross-sectional areas and mean T2 and ADC were measured in individual fascicles of the tibial and fibular (peroneal) portions of the sciatic nerve at its bifurcation and 10 mm distally. Disease severity was measured using Charcot–Marie–Tooth Examination Score (CMTES) version 2 and compared to imaging findings.

Results: We demonstrated the feasibility of 7T MRI of the proximal sciatic nerve in patients with CMT1A. Using the higher field, it was possible to measure individual bundles in the tibial and fibular divisions of the sciatic nerve. There was no apparent correlation between diffusion measures and disease severity in this small cohort.

Discussion: This pilot study indicated that high-resolution MRI that allows for combined anatomical and quantitative imaging in one scan is feasible at 7T field strengths and can be used to investigate the microstructure of individual nerve fascicles.

KEYWORDS

7T MRI, CMT1A, outcome measures, peripheral nerve imaging

1 | INTRODUCTION

There has been growing interest in contemporary imaging techniques such as magnetic resonance imaging (MRI) to further the evaluation of peripheral nerves, especially amongst patients with hereditary neuropathies.^{1–4} The association between disease chronicity, severity, and nerve volume in patients with hereditary and chronic inflammatory neuropathies has been explored using conventional and quantitative imaging techniques.^{5–9} With the advent of higher resolution imaging, it has become possible to not only obtain diffusion microscopic evaluation of small axons, but also reliably estimate axonal loss and demyelination.¹⁰ Imaging protocols allowing visualization of sciatic nerve fascicles at 3T field strengths have been proposed,¹¹ but the small voxel size required can inherently make imaging with high signal-to-noise ratio (SNR) challenging. Furthermore, quantitative maps are often acquired at lower resolution and can contain artifacts such as distortion, causing challenges in quantitative assessment of individual fascicles. More recently, feasibility of 7T MR imaging was demonstrated in distal tibial nerve fascicular structures.¹² Combining such high-resolution anatomic imaging with quantitative imaging at the same resolution would satisfy a need to simultaneously probe fascicle morphology and microstructure in patients with nerve disease, enabling a holistic image-based assessment of both these factors to aid the clinician in assessing the patient condition and potentially providing biomarkers for the level of pathology.

The aim of this pilot study was to investigate the feasibility of 7T MR imaging in assessment of nerve fascicles of patients with the most common form of hereditary neuropathy, Charcot-Marie-Tooth disease type 1A (CMT1A).

2 | METHODS

2.1 | Patient recruitment

Six patients with genetically confirmed CMT1A participated in the study. The study was approved by the Mass General Brigham Human Research Committee Institutional Review Board (IRB). All study participants provided informed consent. The senior author (R.S.) examined the patients and completed the Charcot-Marie-Tooth Examination Score (CMTES) version 2.

2.2 | Imaging protocol

All patients underwent imaging on a high-field 7T MRI scanner (Terra, Siemens Healthineers) using a 28-channel transmit-receive knee coil (QED). Scans were performed using the double-echo in steady-state (DESS) sequence, a 3D gradient-spoiled MRI sequence known to provide good musculoskeletal tissue contrast with high signal-to-noise ratio (SNR) efficiency and minimal distortion.¹³ This sequence acquires two MRI signals during each repetition time (TR), one before a spoiler gradient and one after, giving different contrasts.¹⁴ Due to the steady-state nature of the imaging sequence, both signals contain contributions from

several past repetition times, representing a range of spin histories and decay durations. In our implementation, the two acquired signals were processed separately and reconstructed into two images.¹⁵ We performed axial scans with an in-plane resolution of $0.1483 \times 0.1483 \text{ mm}^2$ and a field of view (FOV) of $140 \times 140 \text{ mm}^2$, TR = 22.5 ms, echo time (TE) = 6.3 ms, flip angle = 20° , 80.2-mm thick slices, readout bandwidth = 195 Hz/pixel, anterior/posterior phase encoding direction, and $2 \times$ parallel imaging, resulting in a scan time of 11.5 min. To obtain diffusion estimates, the sequence was run twice, once with low diffusion weighting and once with high diffusion weighting (obtained by using a small and large spoiler gradient moment of 12 and 157 $\text{ms}^* \text{mT/m}$, respectively). The spoiler direction, providing the diffusion sensitivity, was along the superior/inferior axis and thus in the slice direction. While the diffusion decay is not exponential and thus does not have a traditional b -value, the sensitivity of the scan with the larger gradient was estimated to correspond to approximately $b = 400 \text{ s/mm}^2$ in a conventional diffusion weighted scan, while the other scan can be well approximated to have no diffusion weighting. By obtaining the quantitative estimates from the same DESS sequence that produces the anatomic images, undistorted maps can be obtained at a high resolution suitable for fascicle analysis, allowing easy co-registration with anatomy. A 1–2–1 binomial water-selective radiofrequency pulse was used to suppress the signal from fat.

2.3 | Data processing

By comparing the two DESS echoes to theoretical models,¹⁶ a T2 map and a map of the apparent diffusion coefficient (ADC) was computed for the participants. This was achieved by computing theoretical predictions of the ratios of different signal combinations over a range of T2 and ADC and storing them in a digital dictionary. Then, the measured signal ratios for each individual pixel were compared to the entries in the dictionary, the best match found, and the corresponding T2 and ADC values determined as the estimate for that pixel. The T2 value was double-checked against another known method that only produces T2¹⁷ to confirm the two methods gave the same result. In this analysis, T1 was assumed to be 1.2 s, although the methodology has low sensitivity to this parameter. A slice was then located in each patient that contained the sciatic nerve, just before its bifurcation into the tibial and fibular (peroneal) nerves. In this sample slice, regions of interest (ROIs) were drawn in individual fascicles of the first DESS echo and then copied over to the quantitative maps. The fascicle cross-sectional areas and mean T2 and ADC were measured in individual fascicles. Another slice, 10 mm distally away from the first slice, was then examined and a similar ROI analysis performed, but this time, the axons in the tibial and fibular nerves were analyzed separately.

3 | RESULTS

The high resolution and image quality of the 7T scanner, the 28-channel coil, and the DESS sequence enabled undistorted

TABLE 1 Clinical and imaging results for the patients for sciatic, tibial, and fibular nerves across all six patients

Sciatic nerve								
Subject	Age (year)	Gender	CMTES Score	Fascicle area [mm ²]	Fascicle T2 [ms]	Fascicle ADC [μm ² /ms]	Fascicle numbers	Total area [mm ²]
1	40	F	10	3.0 [0.2;12.0]	42.1 [33.8;53.0]	1.4 [0.7;1.9]	14	42.4
2	40	M	12	1.9 [0.3;13.0]	35.5 [24.7;47.4]	1.3 [0.4;2.0]	34	64.2
3	24	F	8	1.0 [0.3;4.0]	41.7 [34.9;52.5]	1.3 [0.7;2.2]	20	19.1
4	63	F	12	0.9 [0.2;1.8]	36.3 [28.6;48.3]	0.9 [0.4;1.6]	35	33.0
5	29	F	8	1.8 [0.1;4.3]	27.8 [21.4;40.5]	1.3 [0.6;2.3]	24	42.8
6	25	M	5	2.9 [0.4;9.0]	29.4 [24.1;34.3]	0.3 [0.2;0.4]	29	83.2
Tibial nerve								
Subject	Age (year)	Gender	CMTES Score	Fascicle area [mm ²]	Fascicle T2 [ms]	Fascicle ADC [μm ² /ms]	Fascicle numbers	Total area [mm ²]
1	40	F	10	2.5 [0.6;5.3]	40.8 [29.8;52.8]	1.6 [1.0;2.1]	11	27.2
2	40	M	12	1.1 [0.3;2.5]	36.3 [27.8;52.4]	1.4 [0.7;2.3]	33	36.1
3	24	F	8	1.0 [0.4;4.2]	38.1 [33.9;47.3]	1.0 [0.6;1.7]	16	15.5
4	63	F	12	1.5 [0.3;3.8]	38.5 [30.6;52.8]	0.8 [0.5;1.2]	18	27.4
5	29	F	8	1.6 [0.2;4.7]	27.7 [24.2;35.8]	1.5 [0.8;3.1]	17	26.8
6	25	M	5	4.0 [0.9;7.2]	29.5 [25.2;35.7]	0.3 [0.2;0.3]	16	64.3
Fibular nerve								
Subject	Age (year)	Gender	CMTES Score	Fascicle area [mm ²]	Fascicle T2 [ms]	Fascicle ADC [μm ² /ms]	Fascicle numbers	Total area [mm ²]
1	40	F	10	3.0 [1.6;4.8]	40.6 [38.2;43.8]	1.9 [1.6;2.2]	4	12.1
2	40	M	12	5.2 [0.6;22.3]	43.1 [38.1;51.0]	2.5 [1.9;3.0]	5	26.2
3	24	F	8	1.4 [0.5;2.6]	39.7 [32.1;49.9]	1.5 [0.9;2.3]	6	8.1
4	63	F	12	1.2 [0.4;2.0]	35.3 [31.2;45.7]	0.8 [0.5;1.3]	15	17.5
5	29	F	8	4.3 [0.5;15.5]	27.8 [26.5;30.2]	1.6 [1.2;2.0]	4	17.0
6	25	M	5	3.6 [0.8;9.3]	26.1 [23.3;27.7]	0.3 [0.2;0.4]	9	32.1

Note: When applicable, values are reported as mean [95 percentile interval].

Abbreviations: ADC, apparent diffusion coefficient; CMTES, Charcot-Marie-Tooth examination score; F, female; M, male; mm², square millimeters; ms, milliseconds; μm², square micrometers.

visualization and quantitative measurements of individual fascicles (Table 1). Using the higher field, it was possible to measure individual bundles in the tibial and fibular divisions of the sciatic nerve. The epineurium could be well visualized in most patients (Figure 1). Figure 2 shows the distribution of fascicle T2 in each of the patients.

4 | DISCUSSION

In this pilot study, the results indicate that 7T SNR improvements may allow better study of the structure of nerve fascicles and provide accurate quantitative estimation of tissue characteristics such as relaxation and diffusivity. These methods may help to not only gain more insight to nerve morphology but also help better understand microstructural aspects and function.

The high resolution and low image distortion in this study's methodology enabled reliable co-registration of quantitative values with underlying anatomy. Additionally, visualizing the epineurium may aid

in delineating the area of the whole nerve by drawing a region of interest, further enabling manual and automatic software-based nerve segmentation approaches. It should be noted that for very small fascicles, even a small number of erroneous pixels due to noise or other factors can greatly affect the mean value for that fascicle, potentially creating outliers as in Figure 2. Currently, there is no established method to discern nerve fascicles from vessels, vasa nervosum, or other connective tissues, which could be a potential source of noise in the data. Theoretically, improvement in the resolution of the diffusion imaging protocol may help differentiate between different types of fascicles and vessels. The ability to do both morphological and quantitative measurements at the fascicle level may yield better resolution of individual nerve pathology compared to examination of the entire nerve including tissue between fascicles.

T2 relaxation is a common measure in MR, describing how fast the signal decays due to spin-spin interaction. T2 relaxation has been explored as a biomarker for estimating the breakdown of the extracellular matrix in cartilage,¹⁸ muscle inflammation,¹⁹ and peripheral

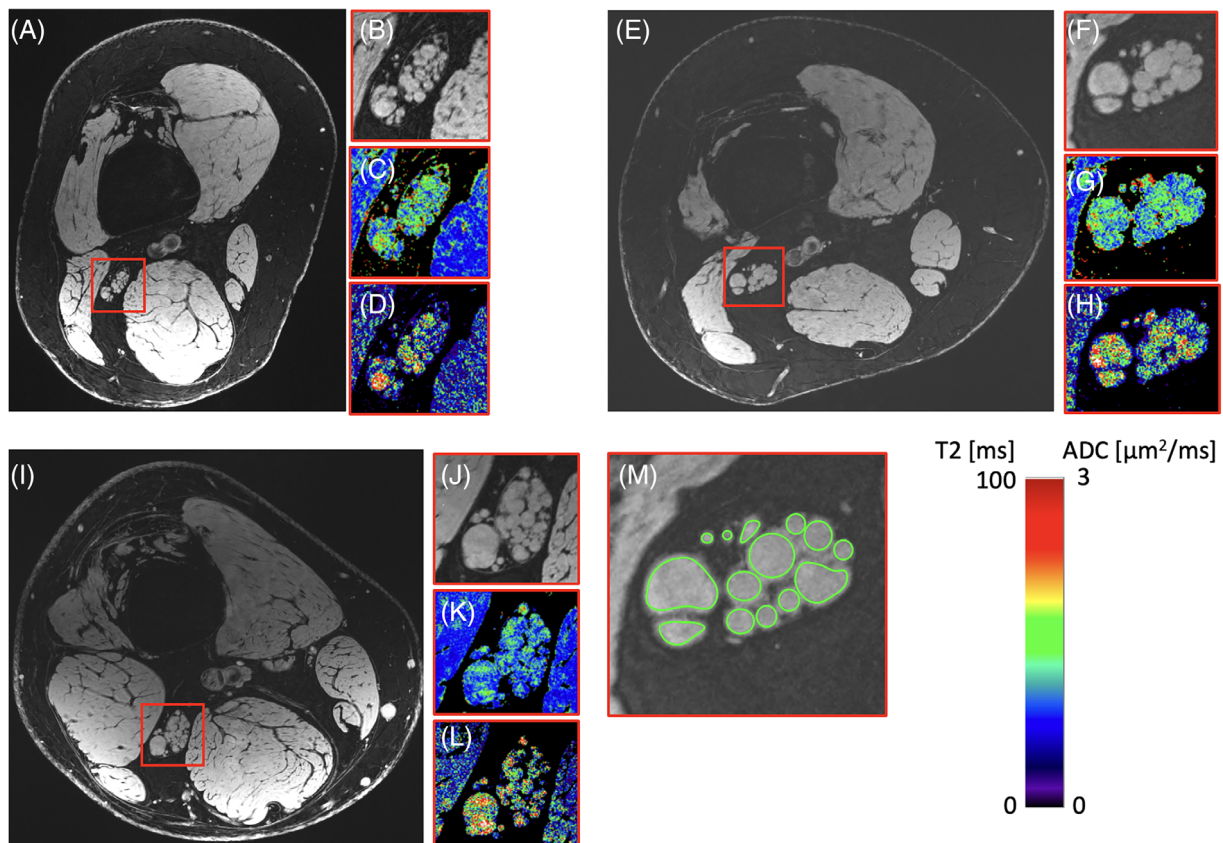


FIGURE 1 A,E,I, Sciatic nerve images of CMT1A patients 3, 1, and 2 in Table 1, with CMTES scores 8, 10, and 12, respectively. B,F,J, A zoomed-in region showing the sciatic nerve in more detail. Note that the epineurium is well visible in panels B and J. C,G,K, A T2 map of the zoomed-in region. D, H, L, ADC map of the same region. M, An example of the ROIs drawn in the anatomical image (for the patient in figures E–H), covering each fascicle, with the average quantitative value for each fascicle recorded by analyzing the ROIs in the corresponding map

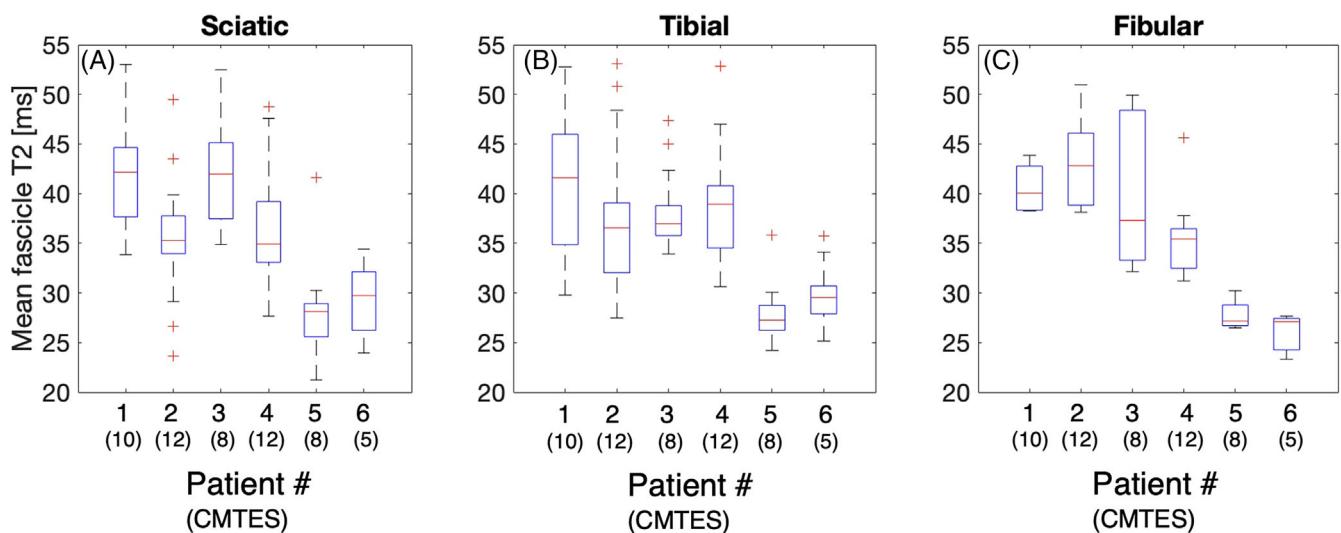


FIGURE 2 A,B,C, Box plots showing the distributions of fascicle T2 values measured in the sciatic, tibial, and fibular nerve, respectively, acquired as shown in Figure 1M, for all six patients. The central mark signifies the median, the box edges are the 25th and 75th percentiles, the whiskers represent the whole distribution excluding outliers, and the red crosses signify outliers

nerves.^{20–22} T2 relaxation in a relatively bidirectional structure such as a peripheral nerve could represent the degree of structural integrity.²³ The ability to estimate T2 in single fascicles, in combination

with anatomical images acquired concurrently, presents a future direction of using fascicle size and T2 value in a complimentary manner for assessing the health of peripheral nerves and surrounding muscles.

Compared to lower-field MR imaging, peripheral nerve T2 has been measured to have significantly shorter relaxation times at 7T.²² Prior studies have indicated higher nerve T2 in patients at 7T but not at 3T.^{24,25} This study also included ADC measurements, previously found to be elevated in CMT1A,²⁵ but we acknowledge that such steady-state measurements are known to be susceptible to field imperfections, not corrected for in this study, which may contribute to some of the observed variability (Table 1).

This is a very small feasibility study of patients with mild to moderate disability, not powered to provide validated biomarkers or statistical correlation with clinical measures. There are multiple potential confounders beyond disease severity, including chronicity and concomitant processes.⁶ Larger scale case-control, longitudinal studies including more severely affected patients, and validation of the imaging protocol with conventional methods such as spin-echo imaging could serve as future steps to better evaluate the utility of these measures. Last, 7T imaging technology is currently available at only a small number of centers, limiting generalizability of such techniques for more widespread use.

Ultimately, improved quantitative techniques may serve to monitor the efficacy of treatments by identifying meaningful anatomic changes that may precede evident clinical improvement.

ACKNOWLEDGMENTS

This study is supported by a grant from American Academy of Neurology clinical research scholarship (American Brain Foundation and Muscle Study Group). Imaging was performed at the Athinoula A. Martinos Center for Biomedical Imaging at the Massachusetts General Hospital using resources provided by the Center for Functional Neuroimaging Technologies (P41EB015896) and the Center for Mesoscale Mapping (P41EB030006), Biotechnology Resource Grants supported by the National Institute of Biomedical Imaging and Bioengineering, National Institutes of Health (NIH). The NIH also provided support through grants K99AG066815, R01EB027779, and R01EB028797. The content is solely the responsibility of the authors and does not necessarily represent the official views of the NIH.

CONFLICT OF INTEREST

The author reports no relevant financial disclosure or conflict of interest.

DATA AVAILABILITY STATEMENT

The data that support the findings of this study are available from the corresponding author upon reasonable request.

ETHICAL PUBLICATION

We confirm that we have read the Journal's position on issues involved in ethical publication and affirm that this report is consistent with those guidelines.

ORCID

Daniel J. Park  <https://orcid.org/0000-0002-7263-9327>

Reza Sadjadi  <https://orcid.org/0000-0003-3829-6030>

REFERENCES

1. Aagaard BD, Maravilla KR, Kliot M. MR neurography. MR imaging of peripheral nerves. *Magn Reson Imaging Clin N Am*. 1998;6:179-194.
2. Chhabra A, Williams EH, Wang KC, Dellon AL, Carrino JA. MR neurography of neuromas related to nerve injury and entrapment with surgical correlation. *AJNR Am J Neuroradiol*. 2010;31:1363-1368.
3. Dailey AT, Tsuruda JS, Filler AG, Maravilla KR, Goodkin R, Kliot M. Magnetic resonance neurography of peripheral nerve degeneration and regeneration. *Lancet*. 1997;350:1221-1222.
4. Lehmann HC, Zhang J, Mori S, Sheikh KA. Diffusion tensor imaging to assess axonal regeneration in peripheral nerves. *Exp Neurol*. 2010;223:238-244.
5. Tanaka K, Mori N, Yokota Y, Suenaga T. MRI of the cervical nerve roots in the diagnosis of chronic inflammatory demyelinating polyradiculoneuropathy: a single-institution, retrospective case-control study. *BMJ Open*. 2013;3:e003443.
6. Tazawa K, Matsuda M, Yoshida T, et al. Spinal nerve root hypertrophy on MRI: clinical significance in the diagnosis of chronic inflammatory demyelinating polyradiculoneuropathy. *Intern Med*. 2008;47:2019-2024.
7. Ishikawa T, Asakura K, Mizutani Y, et al. MR neurography for the evaluation of CIDP. *Muscle Nerve*. 2017;55:483-489.
8. Chhabra A, Carrino JA, Farahani SJ, et al. Whole-body MR neurography: prospective feasibility study in polyneuropathy and Charcot-Marie-Tooth disease. *J Magn Reson Imaging*. 2016;44:1513-1521.
9. Fortanier E, Ogier AC, Delmont E, et al. Quantitative assessment of sciatic nerve changes in Charcot-Marie-Tooth type 1A patients using magnetic resonance neurography. *Eur J Neurol*. 2020;27:1382-1389.
10. Assaf Y, Blumenfeld-Katzir T, Yovel Y, Basser PJ. AxCaliber: a method for measuring axon diameter distribution from diffusion MRI. *Magn Reson Med*. 2008;59:1347-1354.
11. Chen Y, Haacke EM, Li J. Peripheral nerve magnetic resonance imaging. *F1000Res*. 2019;F1000 Faculty Rev-1803:8.
12. Yoon D, Biswal S, Rutt B, Lutz A, Hargreaves B. Feasibility of 7T MRI for imaging fascicular structures of peripheral nerves. *Muscle Nerve*. 2018;57:494-498.
13. Gold GE, Hargreaves BA, Reeder SB, et al. Balanced SSFP imaging of the musculoskeletal system. *J Magn Reson Imaging*. 2007;25:270-278.
14. Redpath TW, Jones RA. FADE—a new fast imaging sequence. *Magn Reson Med*. 1988;6:224-234.
15. Staroswiecki E, Granlund KL, Alley MT, Gold GE, Hargreaves BA. Simultaneous estimation of T(2) and apparent diffusion coefficient in human articular cartilage in vivo with a modified three-dimensional double echo steady state (DESS) sequence at 3T. *Magn Reson Med*. 2012;67:1086-1096.
16. Weigel M. Extended phase graphs: dephasing, RF pulses, and echoes—pure and simple. *J Magn Reson Imaging*. 2015;41:266-295.
17. Sveinsson B, Chaudhari AS, Gold GE, Hargreaves BA. A simple analytic method for estimating T2 in the knee from DESS. *Magn Reson Imaging*. 2017;38:63-70.
18. Mosher TJ, Dardzinski BJ. Cartilage MRI T2 relaxation time mapping: overview and applications. *Semin Musculoskelet Radiol*. 2004;8:355-368.
19. Maillard SM, Jones R, Owens C, et al. Quantitative assessment of MRI T2 relaxation time of thigh muscles in juvenile dermatomyositis. *Rheumatology (Oxford)*. 2004;43:603-608.
20. Chappell KE, Robson MD, Stonebridge-Foster A, et al. Magic angle effects in MR neurography. *AJNR Am J Neuroradiol*. 2004;25:431-440.
21. Maeda A, Suzuki T, Hayakawa K, Funahashi T, Kuroiwa T, Fujita N. T2 mapping of the median nerve in patients with carpal tunnel syndrome and healthy volunteers. *Muscle Nerve*. 2021;63:774-777.

22. Gambarota G, Veltien A, Klomp D, Van Alfen N, Mulkern RV, Heerschap A. Magnetic resonance imaging and T2 relaxometry of human median nerve at 7 tesla. *Muscle Nerve*. 2007;36:368-373.
23. Takagi T, Nakamura M, Yamada M, et al. Visualization of peripheral nerve degeneration and regeneration: monitoring with diffusion tensor tractography. *NeuroImage*. 2009;44:884-892.
24. Riegler G, Drlicek G, Kronnerwetter C, et al. High-resolution axonal bundle (fascicle) assessment and triple-Echo steady-state T2 mapping of the median nerve at 7T: preliminary experience. *Investig Radiol*. 2016;51:529-535.
25. Vaeggemose M, Vaeth S, Pham M, et al. Magnetic resonance neurography and diffusion tensor imaging of the peripheral nerves in

patients with Charcot-Marie-Tooth type 1A. *Muscle Nerve*. 2017;56:E78-E84.

How to cite this article: Sveinsson B, Rowe OE, Stockmann JP, et al. Feasibility of simultaneous high-resolution anatomical and quantitative magnetic resonance imaging of sciatic nerves in patients with Charcot-Marie-Tooth type 1A (CMT1A) at 7T. *Muscle & Nerve*. 2022; 1-6. doi:[10.1002/mus.27647](https://doi.org/10.1002/mus.27647)